HHS Public Access

Author manuscript

Mol Cancer Ther. Author manuscript; available in PMC 2018 September 01.

Published in final edited form as:

Mol Cancer Ther. 2017 September ; 16(9): 1751–1764. doi:10.1158/1535-7163.MCT-17-0040.

CDK4/6 inhibitors sensitize Rb-positive sarcoma cells to Wee1 kinase inhibition through reversible cell cycle arrest

Ashleigh M. Francis[2,*], **Angela Alexander**[1,*], **Yanna Liu**[2], **Smruthi Vijayaraghavan**[1], **Kwang Hui Low**[1], **Dong Yang**[1], **Tuyen Bui**[1], **Neeta Somaiah**[3], **Vinod Ravi**[3], **Khandan Keyomarsi**[1,**], and **Kelly K. Hunt**[2,**]

[1]Department of Experimental Radiation Oncology, The University of Texas MD Anderson Cancer Center, Houston, Texas 77030

[2]Department of Surgical Oncology, The University of Texas MD Anderson Cancer Center, Houston, Texas 77030

[3]Department of Sarcoma Medical Oncology, The University of Texas MD Anderson Cancer Center, Houston, Texas 77030

Abstract

Research into the biology of soft tissue sarcomas has uncovered very few effective treatment strategies that improve upon the current standard of care which usually involves surgery, radiation, and chemotherapy. Many patients with large (>5cm), high-grade sarcomas develop recurrence, and at that point have limited treatment options available. One challenge is the heterogeneity of genetic drivers of sarcomas, and many of these are not validated targets. Even when such genes are tractable targets, the rarity of each subtype of sarcoma makes advances in research slow. Here we describe the development of a synergistic combination treatment strategy that may be applicable in both soft tissue sarcomas as well as sarcomas of bone that takes advantage of targeting the cell cycle. We show that Rb-positive cell lines treated with the CDK4/6 inhibitor palbociclib reversibly arrest in the G1 phase of the cell cycle, and upon drug removal cells progress through the cell cycle as expected within 6–24 hours. Using a long-term high-throughput assay that allows us to examine drugs in different sequences or concurrently, we found that palbociclib-induced cell cycle arrest poises Rb-positive sarcoma cells (SK-LMS1 and HT-1080) to be more sensitive to agents that work preferentially in S-G2 phase such as doxorubicin and Wee1 kinase inhibitors (AZD1775). The synergy between palbociclib and AZD1775 was also validated *in vivo* using SK-LMS1 xenografts as well as Rb-positive patient-derived xenografts (PDX) developed from leiomyosarcoma patients. This work provides the necessary preclinical data in support of a clinical trial utilizing this treatment strategy.

[**]*Co-Corresponding Authors*. Khandan Keyomarsi, PhD, Department of Experimental Radiation Oncology, The University of Texas, MD Anderson Cancer Center, 6565 MD Anderson Boulevard, Unit 1052, Houston, TX 77030 USA, Phone: 713-792-4845, kkeyomar@mdanderson.org, Kelly K. Hunt, MD, Department of Breast Surgical Oncology, The University of Texas, MD Anderson Cancer Center, 1400 Pressler Street, Unit 1434, Houston, TX 77030 USA, Phone: 713-792-7216, khunt@mdanderson.org.

[*]Equal contribution

DEDICATION

This work is dedicated to the memory of ArshiaTabrizi who fought hard, but lost his battle to LMS.

Keywords

cell cycle; sarcoma; CDK4/6; Wee1

Introduction

Sarcomas are a heterogeneous group of malignancies derived from mesenchymal cells that affect both children and adults of all ages and can arise anywhere in the body (1). More than 80 subtypes of sarcomas exist, broadly categorized into soft tissue sarcomas (STS) and primary bone sarcomas, each with significant differences in underlying biology, natural history and treatment paradigms (2–4). Overall, newer treatment strategies for sarcoma patients lag behind many other solid tumors, partly due to the difficulty in performing translational research and clinical trials in selected sarcoma subtypes due to each entity being so rare. Sarcomas account for only 1% of all adult solid tumors and up to 20% of childhood solid tumors. Standard chemotherapy regimens usually consist of doxorubicin-based combinations, and many tumors are aggressive and refractory to, or eventually progress on standard chemotherapy (1, 5). Surgery plays a critical role in local control of primary tumors, along with radiation and chemotherapy in certain histologies that are known to be more sensitive to radiation and/or chemotherapy (6). However, rates of distant metastasis are still high and are the major cause of death in sarcoma patients (3) and newer, more targeted treatments are needed. However, many of the genetic drivers of sarcomas such as the fusion-genes used to define diagnosis are currently undruggable (7, 8). While there are examples of sarcoma subtypes with known active targeted therapies (e.g. tyrosine kinase inhibitors in gastrointestinal stromal tumors, and pazopanib in several STS) there is a paucity of described pathway alterations that can be used to guide treatment (9–12).

Deregulation of the cell cycle is one of the hallmarks of cancer, and may be a reasonable target for the development of new therapies in sarcoma (13). In particular, the G1 checkpoint may be targeted due to the frequent alterations involving cyclin dependent kinases (CDKs) CDK4 and CDK6, p16 and the retinoblastoma (Rb) protein across multiple subtypes of sarcoma (14). CDKs are kinases that regulate the cell cycle, as well as transcription/RNA processing through phosphorylation of substrates such as Rb. CDKs that are involved in the cell cycle are regulated through binding to cyclins, which are transcriptionally regulated by the cell cycle. However, in cancer cyclins such as cyclin D and E can be amplified or overexpressed leading to cell cycle-independent constitutive activation of CDKs that drive cell cycle progression. For this reason, targeting CDKs with small molecule inhibitors has been an area of interest in many malignancies, including sarcoma (13). Although there are currently no approved cell cycle targeted therapies in sarcoma, there is an emerging body of promising preclinical and early clinical trial data that show signs of efficacy. CDK4/6-specific inhibitors are the most clinically advanced type of CDK inhibitor, with palbociclib being the first drug in this class to receive FDA approval in the setting of metastatic estrogen receptor (ER) positive breast cancers given in combination with the aromatase inhibitor letrozole or the selective estrogen-receptor-downregulator fulvestrant (15, 16). Two other CDK4/6 inhibitors, abemaciclib and ribociclib, are undergoing FDA review for approval in a similar setting (17). More recently, these drugs are also being investigated in other solid

tumors ranging from melanoma to non-small cell lung cancer, both as single agents and in combination with other signal transduction inhibitors (18, 19).

CDK4/6 inhibitors have already been examined clinically in well-differentiated and dedifferentiated liposarcomas, which almost universally harbor high-level amplifications of 12q14, the region containing CDK4. High expression of CDK4 has also been associated with a poor prognosis in these patients (14, 20). In a clinical trial with palbociclib in adults with liposarcoma, there was only 1 partial response noted, but the 12-week progression free survival (PFS) rate was 66%. This PFS exceeded the primary endpoint that would be considered a positive signal in sarcoma (21). A follow-up study using a different dose and schedule also resulted in a favorable efficacy signal in this disease, including 1 complete response out of 30 patients (22). The goal of our work was to explore the use of CDK4/6 inhibitors in other sarcoma subtypes and to determine whether they may be used to synchronize tumor cells in the G1 phase of the cell cycle, positioning them to enter S and G2/M phase synchronously where they would be more responsive to G2/M kinase inhibitors.

One such G2/M target, Wee1 kinase, is a key regulator of the G2/M checkpoint, through inhibitory phosphorylation of CDK1, preventing progression of cells with DNA damage into mitosis (23). Wee1 kinase inhibitors have been found to synergize with DNA damaging chemotherapies (such as platinum agents or gemcitabine) or radiation in many cancer cell lines due to promoting premature mitosis in cells with lethal DNA damage, leading to cell death via mitotic catastrophe. In this report, we tested the hypothesis that palbociclib-induced G1 arrest and subsequent release primes the cells to respond to agents that are active maximally in S/G2 phase such as Wee1 kinase inhibitors. To this end, we interrogated the utility of the sequential combination treatment of palbociclib followed by AZD1775 (24) in sarcomas using *in vitro* and *in vivo* (cell line and patient derived xenografts) model systems.

Materials and Methods

Cell culture and reagents

Sarcoma cell lines were acquired from ATCC, and cultured as indicated in Supplemental Table 1. All cell lines were authenticated by STR profiling upon receipt. Large batches of cells were frozen down so that cells could be maintained in culture for no more than 6 weeks for experiments. Palbociclib was a generous gift from Pfizer Oncology (New York, NY) and AZD1775 was purchased from Proactive Molecular Research (Alachua, FL).

Western blot analysis

Western blot analyses were performed as previously described with the following modifications. The cell pellet was sonicated in phosphate buffered saline (PBS) containing a cocktail of protease/phosphatase inhibitors (25 g/mL leupeptin, 25 g/mL aprotinin, 10 g/mL pepstatin, 1 mM benzamidine, 10 g/mL soybean trypsin inhibitor, 0.5 mM phenylmethylsulfonyl fluoride, 50 mM sodium fluoride, and 0.5 mM sodium orthovanadate). The primary antibodies used were phospho-Rb Ser-780 (Cell Signaling #9307), Rb (Cell Signaling #9309), CDK4 (Santa Cruz sc-260), CDK6 (Santa Cruz sc-177), p16 (Santa Cruz sc-1207), E2F1 (Santa Cruz sc-251), Beta actin (Millipore MAB1501),

PARP (Cell Signaling #9542), Caspase 3 (Cell Signaling #9662), and Vinculin (Sigma V9131).

Cell cycle analysis

The cell cycle was analyzed using propidium iodide (PI) staining and flow cytometry analysis using standard methods. Briefly, cells were plated and treated as indicated in the text describing each figure. At the end of treatment, cells were harvested by trypsinization and fixed in 70% ethanol (in PBS). Following fixation and rinsing with PBS, cells were stained with 1 μg/mL PI in buffer overnight. The staining buffer consisted of PBS + 0.5% Tween-20 and 0.5% bovine serum albumin with 20 μg/mL RNase A. A FACSCalibur flow cytometer was used with data generated using CellQuest Pro software, version 6.0.2 (BD Biosciences).

Generation of shRNA-expressing cells

To generate the SK-LMS1 shRNA cells, we used lentiviral transduction of shRNA plasmids. HEK293T cells were transfected using PEI at a 3:1 ratio with the shRNA, and packaging vectors. Media was replaced on day 2, and supernatant containing virus collected on day 3 and day 4. Viral infection was allowed to proceed for 24 hours. Puromycin was used to select for transduced cells, however, after selection cells were maintained in regular DMEM:F12 media. The Rb shRNAs used were V3LHS_340825 and V3LHS_340827 (Dharmacon) and the non-targeting control was Cat#- RHS 4346, sense sequence-CTCGCTTGGGCGAGAGTAA (Open Biosystems).

High throughput survival assay (HTSA)

This 96-well format high-throughput screening assay was performed with minor changes to previously published protocols from our lab. The density for each cell line was optimized using growth curves prior to beginning single drug treatments (listed in Supplemental Table 1). The changes to the timeline for this assay are shown as a schematic in Supplemental Figure 3A, due to the slow mechanism of action of palbociclib necessitating 6 days of treatment. After palbociclib treatment, fresh media containing no drugs was used for “recovery” to allow cells to re-enter the cell cycle. The concentrations of each drug used for combinations are listed in Supplemental Table 2.

Measurement of senescence

Senescence was measured by the senescence-associated galactosidase (SA-β gal) staining kit (Millipore, Billerica, MA) according to the manufacturer’s standard protocol. Briefly, cells were plated at a low density of 2,000 to 4,000 cells (depending on the plating efficiency of the cell line) in each well of 12-well plates and treated as described for HTSA (see Supplemental Figure 3A). Following drug treatments and recovery, cells were then washed with PBS, fixed, and stained with SA-β gal solution overnight. The cells were then photographed using the Evos XL Core cell imaging system (ThermoFischer, Waltham, MA) and senescent cells were quantified by counting 100 cells in three different fields for each replicate. A minimum of three technical and three biological replicates were performed for each condition.

Mouse Xenografts

All mouse experiments were performed under IACUC approved protocols at the University of Texas MD Anderson Cancer Center. Briefly, 1×10^6 SK-LMS1 cells were injected subcutaneously into 4–5 week old male nude mice, and randomized into treatment groups once the tumors reached 200 mm^3. Palbociclib was dissolved in sterile 50 mM sodium lactate buffer, and AZD1775 was dissolved in 0.5% methylcellulose. Palbociclib was administered by oral gavage daily (70mg/kg for combination treatment experiments), and AZD1775 was administered twice daily (70mg/kg) also by oral gavage. PDX lines were generated from surgical samples under an IRB approved protocol (LAB07-0659). PDX lines were generated using established methods, and the patient details can be found in Supplemental Table 3. PDX model 22 was used for assessment of the efficacy of palbociclib and AZD1775 as single agents and in combination. To propagate enough tumor to allow for the 4 treatment arm experiment (Figure 6C–6E), PDX model 22, was passaged into the flanks of 10 nude mice. Once the tumors reached 1.5 cm^3, they were excised and cut into 30 mm^3 segments and transplanted into the flanks of 20 nude mice. Mice were randomized (when tumors reached 150 mm^3), into 4 treatment arms (5 mice/arm) using the same treatment strategy as in the SK-LMS1 experiments. Animals were weighed weekly to document toxicity, and tumors were measured in 2 dimensions using calipers. Tumor volumes were calculated using the formula $\pi/6 * L * W^2$. Tissues were fixed in 10% neutral buffered formalin for 24 hours and then transferred into 70% ethanol prior to processing for paraffin blocks.

BrdU Immunohistochemistry

To assess the recovery of SK-LMS1 xenograft cells into active cell cycle post-treatment with palbociclib, mice were injected intraperitoneally with 0.25 mg/g body weight of BrdU 2 hours before euthanasia. Paraffin-embedded sections of the tumors were deparaffinized and rehydrated, and antigen retrieval performed using 10 mM sodium citrate (pH=6). Rat anti-BrdU monoclonal antibody (GeneTex clone BU1/75, GTX26326) was used at a dilution of 1:500 for staining, and slides counterstained with Hematoxylin, Mayer's (Lillies's modification, from DAKO). Two representative images per slide were taken under a 40× objective lens, and BrdU cells counted manually, including an average of 400–800 cells per animal.

Statistical analysis

All experiments were performed with a minimum of three technical and three biological replicates, and values reported are the mean of the three biological replicates, unless otherwise indicated. Error bars represent the standard deviation from the mean, unless otherwise indicated. Pairwise comparisons were analyzed using multiple *t*-tests (one unpaired *t*-test per row). For all tests, differences were considered statistically significant at a p-value of 0.05 or less. For all figures, ns: $p>0.05$; *$p<0.05$; **$p<0.01$; ***$p<0.001$; ****$p<0.0001$. All statistical analyses were performed using the GraphPad Prism software.

Results

Breast cancer studies have demonstrated that cell lines that are most sensitive to CDK4/6 inhibitors are the ER-positive cell lines, most of which retain wild-type Rb (25). However, in sarcoma the utility of Rb as a predictive biomarker has not been established. Therefore, to select both Rb-positive and Rb-negative cell lines for analysis of drug sensitivity and cell cycle profiling, we subjected a panel of soft tissue and primary bone sarcoma cell lines to western blot analysis for Rb and related G1 checkpoint proteins (Figure 1A). From this analysis, we found that SaOS2 (osteosarcoma) completely lacks Rb expression, and Rb is expressed at a low level in RD cells (rhabdomyosarcoma). All other cell lines expressed abundant Rb protein, which was also phosphorylated since we harvested actively cycling cells. CDK4 and CDK6 are highly expressed in all of the cell lines we tested, as is cyclin D1. We also found that 4 of the 6 cell lines do not express significant levels of p16, whereas SaOS2 and RD express p16. From these cell lines, we selected HT-1080 (fibrosarcoma) and SK-LMS1 (leiomyosarcoma) as representative Rb-positive, p16-negative cell lines and RD and SaOS2 as Rb-negative/low cell lines. We also used U2OS (osteosarcoma) as another Rb-positive cell line in many i*n vitro* experiments to confirm our results.

CDK4/6 inhibitors approved for patients with hormone-receptor positive breast cancers have been shown to work more efficiently in cell lines that have intact G1 checkpoint function (i.e. Rb present). We confirmed this relationship holds true in sarcoma cell lines as well using a modification of our previously-described high-throughput survival assay (26), treating cells with palbociclib (PD) for different time intervals (Figure 1B and Supplemental Figure 1A). Both Rb-positive cell lines (HT-1080, SK-LMS1 and U2OS) show a time-dependent increase in sensitivity to palbociclib, whereas Rb-negative cell lines (RD and SaOS2) require significantly higher doses (i.e. > 5μM) that are not pharmacologically achievable *in vivo* to significantly inhibit growth (Figure 1B and Supplemental Figure 1B).

Since CDK4/6 inhibitors have been shown to be largely cytostatic due to causing G1 cell cycle arrest, in aggressive malignancies such as sarcomas, combination treatments with other agents are likely needed for significant tumor response. We hypothesized that inducing a reversible G1 arrest with CDK4/6 inhibitors, then allowing recovery and re-entry into the cell cycle, may prime cells for sensitivity to agents that preferentially act during S or G2 phase, such as DNA damaging chemotherapy or Wee1 kinase inhibitors. As a first step prior to testing the effect of combination treatment, we examined the sensitivity of cells to doxorubicin, since many standard first-line chemotherapy regimens are doxorubicin-based, and a Wee1 kinase inhibitor (AZD1775). In contrast to palbociclib, Rb status did not predict sensitivity to AZD1775 or doxorubicin, and 1 and 2 days of treatments with either agent resulted in similar dose response curves, independent of Rb status (Figure 1C and D and Supplemental Figure 1C–F).

It is well-established that palbociclib induces a G1 arrest with concomitant S phase reduction in many cancer cell lines by continuous inhibition of CDK4/6 over several population doubling times (27, 28). We confirmed this in our sarcoma model systems using 6 days of treatment, as this was the period of treatment necessary to see consistent strong anti-proliferative effects with an IC50 within the pharmacologically achievable range (29).

Rb-proficient cell lines treated with physiologically relevant doses of palbociclib arrested in G1, whereas Rb-deficient cells did not (Figure 2A, Supplementary Figure 2A). Further, increasing the dose of palbociclib in SaOS2, Rb-negative cells, not only failed to increase the proportion of cells in G1 phase, but also resulted in a modest increase in G2 phase, suggesting off target effects of palbociclib at high doses (Figure 2B). We next addressed the reversibility of the G1 arrest, by treating all 5 cell lines with palbociclib, and then removing the drug and harvesting cells for flow cytometry analysis at several time intervals to determine the time needed to progress to S and G2/M phases of the cell cycle. These analyses revealed that in SK-LMS1 andHT-1080 cells, the cells entered S phase within 6–9 hours of drug removal (Figure 2C, top panels). Similar transitions to S and G2/M were observed in U20S cells (Supplemental Figure 2B). However, in the Rb-low/Rb-negative cells that did not arrest in G1, drug removal did not induce significant changes in S/G2 phase proportions at any concentration of palbociclib used during the course of the study.

To further investigate Rb as a biomarker of palbociclib response, we generated SK-LMS1 cells stably expressing Rb shRNAs, and examined if Rb is necessary and sufficient for palbociclib mediated G1 arrest. Knockdown of Rb did not significantly affect the expression of CDK4, CDK6 or Wee1 kinase as compared to the non-targeting shRNA control cells (Figure 3A). To rule out proliferation differences as an explanation for phenotypic changes, we conducted growth curves with the cell lines. The doubling time for the Rb knockdown cells (KD1 and KD2) were not different from non-targeting control (NTC) (NTC -12.55hrs, KD1 -13.95hrs and KD2 - 14.71hrs) (Figure 3B). We next subjected these cells to palbociclib treatment for 4, 6 and 8 days similar to previous experiments, and examined survival on day 13, as well as counted surviving cells at the end of 6 days of treatment. Rb knockdown cells were 1.5–4 fold more resistant to palbociclib depending on treatment duration and dose (Figure 3C–D), compared to the NTC cells. To determine the requirement for Rb in mediating G1 arrest, we also examined the cell cycle profiles following 6 days of treatment, and found that Rb knockdown cells had moderately less G1 arrest than the control cells (Figure 3E). We also examined the sensitivity of the cell line panel to AZD1775, and as expected found no significant difference indicating that Rb expression does not affect the activity of Wee1 kinase inhibitors (Figure 3F). These results suggest that expression of Rb is necessary for inducing G1 arrest by palbociclib at physiologic concentrations.

Sequential Combination Treatment

Combination treatment efficacy was evaluated using our high-throughput survival assay (HTSA), which allows comprehensive evaluation of 2 or more drugs either in sequence or given concomitantly in any adherent cell line in a 96-well format (schematically depicted in Supplemental Figure 3A). For palbociclib, we selected 6 days of treatment, followed by 6 or 9 hours of recovery in drug free medium, followed by treatment with the second drug (doxorubicin or AZD1775) for 48 hours, and quantification of cell survival at the end of the experiment on day 13. Doses and conditions for each cell line and each drug are listed in Supplemental Tables 1 and 2. Combination indices were calculated using Calcusyn software using the median effect models described by Chou and Talalay (30). The absolute value of the combination index (CI) determines the degree of synergy or antagonism of drug combinations, CIs below 0.9 represent synergism and above 1.1 represent antagonistic

interaction of two agents. Combination treatment with palbociclib followed by doxorubicin (Figure 4A) and palbociclib followed by AZD1775 (Figure 4B) resulted in synergistic activity of the combination in SK-LMS1 and HT-1080 cells, but not in Rb-deficient RD and SaOS2 cells (compare blue to red bars in Figure 4A and 4B). We also compared the effectiveness of concomitant treatment with palbociclib and AZD1775 in SK-LMS1 cells, and observed antagonism at all doses of palbociclib when treating with both drugs on day 1 or day 3 (Supplemental Figure 3D). To address the role of the fresh media recovery period, we performed side-by-side experiments comparing 6 hours recovery to no recovery in HT-1080 cells. At all doses of palbociclib, the average CI values were lower in the recovery experiment compared with no recovery, indicating that this recovery/cell cycle re-entry is important for maximal synergy between these agents (Supplemental Figure 3E). We also asked if expression of Rb is a prerequisite for synergistic activity of palbociclib and AZD1775. We treated the Rb shRNA SK-LMS1 cells with the combination of palbociclib and AZD1775 and results showed that once Rb is knocked down, the combination treatment did not result in synergistic activity (Supplemental Figure 4).

To examine the mechanism of growth inhibition, we examined cleaved caspase 3 and PARP levels in SK-LMS1 cells treated similarly to the HTSA protocol to determine whether apoptosis occurred following combination treatment. The results revealed that apoptosis is not the main mechanism of synergism between these two agents (Supplemental Figure 5). Next, we asked if palbociclib induces senescence in sarcoma cells and if so, would the combination treatment with palbociclib and AZD1775 significantly increase senescence. The rationale for this hypothesis is that treatment of cells (*in vitro* and *in vivo*) with palbociclib alone induces senescence in breast and ovarian cancer cell lines (31, 32). To test this hypothesis, we treated two soft tissue sarcoma cell lines with either single agent or combination therapy with palbociclib and AZD1775 and subjected them to SA-β galactosidase activity measurement (established assay for senescence detection). The data clearly show that while treatment of cells with palbociclib, but not AZD1775, as a single agent causes senescence, the sequential combination treatment of palbocilcib followed by AZD1775 causes significantly more senescence (Figure 4C). Next, we asked if there was DNA damage and/or mitotic catastrophe associated with increased senescence. We measured γ-H2AX (biomarker of DNA double strand breaks) at the end of the treatment and found that while the untreated and single drug treated cells contained discernable γ - H2AX foci, the cells treated with the combination did not have any foci. Upon further examination of the nuclei of those cells, we found that they were undergoing mitotic catastrophe as measured by extent of abnormal nuclei detected by DAPI staining of the remaining cells (Figure 4D). We next measured the percentage of cells with abnormal nuclei and found that in the combination treated cells >30% of cells are undergoing mitotic catastrophe as a result of micro-nucleation (Figure 4D).

In vivo evaluation of sequential treatment with palbociclib followed by AZD1775

Given the synergy observed *in vitro* in Rb-proficient cell lines treated with palbociclib followed by either doxorubicin or AZD1775 (Figure 4), we next interrogated if this sequential combination treatment strategy also results in synergistic activity *in vivo*, using both cell line and patient-derived xenograft (PDX) models. Since doxorubicin is a standard

chemotherapy agent used in the treatment of sarcoma with overlapping toxicity (neutropenia) with palbociclib (29, 33), we focused on AZD1775 as the second drug to provide rationale for a novel dual targeted-therapy trial if preclinical studies proved to be successful. The *in vitro* studies also suggested that the most synergistic schedule of treatment was sequential treatment with palbociclib first, followed by a recovery period so that cells could traverse through S phase, followed by treatment with AZD1775. To recapitulate this *in vitro* scheduling (dose and time) in the *in vivo* design, we first optimized the schedule and dose of palbociclib *in vivo* using SK-LMS1 xenografts (Figure 5B, C). For this experiment, 51 nude (nu/nu strain) mice were injected with 1×10^6 viable SK-LMS1 cells subcutaneously. Tumor burden was measured daily and when the volumes reached 200 mm^3, mice were randomized to 17 arms (3 mice/arm) and were treated with vehicle, 50 mg/kg, 100 mg/kg or 150 mg/kg of palbociclib daily for 3 or 5 days and then allowed to recover for 0, 3 or 6 days. Animals were sacrificed and BrdU staining was performed following the last treatment/recovery period. Treatment of mice with doses higher than 50 mg/kg of palbociclib resulted in inhibition of tumor growth (Figure 5A). BrdU labeling of the tumor tissue revealed that treatment of mice with either 100 mg/kg or 150 mg/kg every day for 5 days was sufficient to significantly inhibit S phase fraction of the cells, and upon recovery for 3 and 6 days, the S phase fraction returned to normal (Figure 5B, 5C). Based on this dose and schedule we next compared single agent to sequential treatment *in vivo* in SK-LMS1 cell line xenografts, and found that under similar dosing schedules, the strategy that was most effective was the sequential combination strategy (Figure 5E, purple line). For this *in vivo* study, we treated cohorts (n=10/cohort) of SK-LMS1 xenografts with the following 4 treatment arms: i) vehicle; ii) palbociclib alone; iii) AZD1775 alone; iv) sequential treatment with palbociclib followed by recovery and treatment with AZD1775. We used a dose of 70 mg/kg/day of palbociclib to minimize toxicity since we treated the mice for 3 cycles of 10 days/cycle (Figure 5D). Results showed that continued administration of palbociclib alone for 3 cycles (5 days on-5 days off) or AZD1775 alone for 3 cycles (2 days on, 8 days off) are not as effective as 3 cycles of sequential combination treatment (5 days palbociclib, recovery for 3 days, followed by 2 days of AZD1775 treatment, Figure 5E). Analysis of tumor samples at the end of the 3 cycles of treatment showed that combination treatment resulted in lower phosphorylation of Rb compared to control or palbociclib treated animals, and also decreased cyclin D1 and E2F1 expression (Figure 5F). Levels of CDK4 and CDK6 were similar in each of the study groups. As we showed *in vitro* (Supplemental Figure 5), markers of apoptosis (caspase 3 and PARP cleavage) were not altered by any of the treatments suggesting that downregulation of Rb is likely the key pathway leading to decreased tumor volume by the combination therapy. To assess the toxicity of the treatments, we recorded the weights of the mice every other day, and observed no significant decreases in weight over time suggesting that the treatment was well-tolerated (Supplemental Figure 6A). These *in vivo* studies with cell line xenografts suggest that sequential treatment with palbociclib, followed by a period of recovery and then treatment with AZD1775 leads to synergistic inhibition of tumor growth.

We next examined the combination treatment strategy *in vivo* using leiomyosarcoma PDX models. We have recently generated PDX models from surgical samples obtained from leiomyosarcoma patients and have established 13 stable PDX lines (Figure 6). To determine

the Rb status of these PDX lines and identify those that would be more likely to respond to sequential treatment with palbociclib ➡ AZD1775 combination therapy, we subjected tumor tissues from the first passage (P1) of each established PDX line to western blot analysis with Rb pathway regulators (Figure 6A). The results revealed that 9 of the 13 PDX models express phospho-Rb protein and that CDK4 and CDK6 were uniformly expressed in the majority of the Rb-positive lines. We also noted that p16 was highly expressed in PDX #6 (no Rb expression) and was not expressed in the PDX lines with the highest phospho-Rb expression (#28 and #18). Since most of the P1 lines can be passaged *in vivo* to multiple passages, we next examined the stability of the Rb pathway in 4 of these PDX models [#18, #20, #21 and #22 (boxed in Figure 6A)] across several passages (Figure 6B). The results revealed that the expression of p16, CDK4 and CDK6 were similar across all passages examined in all 4 PDX models. The one exception was the expression of phosphor-Rb, which was diminished at P3 and P4 in PDX model #21. These results suggest that PDX models #22, #18 and #20 have maintained a stable Rb/CDK axis. The rate of tumor growth of these 4 PDX models over multiple passages are similar to each other and to the SK-LMS1 xenograft model, allowing us to translate our dosing schedule from the SK-LMS1 xenograft model to any of these 4 PDX models. We used PDX model #22 for the *in vivo* treatment study and as with the SK-LMS1 cell line xenografts, we treated cohorts (n=5/cohort) of PDX #20 with the following 4 treatment arms: i) vehicle; ii) palbociclib alone; iii) AZD1775 alone agent; iv) sequential palbociclib followed by recovery and treatment with AZD1775. The PDX model was similarly sensitive to the combination treatment, showing both a significant decrease in tumor growth and final tumor weight at day 25 (Figure 6C–D). Similar to the SK-LMS1 xenograft tumors, phosphorylation of Rb and levels of cyclin D1 were decreased in the combination treated tumors, while levels of CDK4 and CDK6 remained unchanged by the treatment (Figure 6E). To assess the toxicity of the treatments, we recorded the weights of the mice every other day, and observed no consistent decreases in weight over time suggesting that the treatment was well tolerated (Supplemental Figure 6B). Taken together, these results indicate that sequential treatment with palbociclib and AZD1775 is effective in inhibiting leiomyosarcoma growth *in vivo* without significant toxicity, and that Rb is an important mediator of this synergistic activity.

Discussion

Here we identify a novel combination treatment strategy for Rb-positive sarcomas that uses a currently FDA approved drug (palbociclib) to potentiate a newer drug (AZD1775) which is in clinical trials for several solid tumor types (34). This sequential regimen synchronizes cells *in vitro* and *in vivo* to accumulate in G1 phase by treatment with a selective CDK4/6 inhibitor, followed by a period of recovery that allows cells to re-enter the cell cycle where they are more sensitive to subsequent treatment with agents that are active in S phase such as doxorubicin or AZD1775. Our *in vitro* work showed that only Rb-positive cell lines were synergistically inhibited by these treatments, and we directly showed *in vivo* that the palbociclib and AZD1775 combination treatment significantly inhibited tumor growth. We also show that the mechanism by which combination treatment with palbociclib and AZD1775 leads to growth inhibition is through sustained induction of senescence and mitotic catastrophe, but not apoptosis.

The cyclin D1/CDK4/6 pathway is relevant to sarcoma pathogenesis, and hence makes for an ideal therapeutic target. Beyond direct hyperactivation of this growth-promoting pathway through amplification of kinases such as CDK4 in liposarcoma and rhabdomyosarcoma, cyclin D1 may be overexpressed in various subtypes due to oncogenic activation by several transcription factors. For example, in synovial sarcoma the histology-defining fusion chromosome (X;18) creating fusions such as SS18-SSX, results in nuclear expression of β-catenin leading to upregulation of cyclin D1 (35). In alveolar rhabdomyosarcoma, activation of cyclin D1/CDK4 leads to phosphorylation and activation of the signature PAX3-FOXO1 fusion oncogene, known to be important in the aggressiveness of this tumor type (36). Suggesting these sarcoma histologies may be responsive to this novel combinatorial treatment strategy.

Successful clinical translation of the combination regimen of palbociclib and AZD1775 will require careful clinical trial design, both in terms of drug delivery schedule as well as enrollment criteria. Recent trials in STS combining agents with doxorubicin have had mixed results in randomized phase 2–3 trials when all histologic subtypes are included for enrollment, even for agents that have a solid preclinical rationale (37). One agent that has recently been shown to potentiate doxorubicin efficacy is olaratumab (a human PDGFRα monoclonal antibody), which has received FDA approval for use in anthracycline-naïve STS patients in combination with doxorubicin. The approval is based on a phase 2 study showing an 11.8 month improvement in overall survival, however, the mechanism underlying this benefit is not entirely clear (38). One explanation for the mixed clinical results is that there are insufficient validated biomarkers available to select patients for these trials. Our work strongly implicates Rb as a biomarker for CDK4/6 inhibitor combinations, similar to data from other cancer types such as breast cancer and glioblastoma. Selection for enrollment based on biomarkers is more likely to be successful versus the standard approach of enrollment by histologic criteria alone (39). The frequency of Rb positivity within sarcoma appears to differ among histologic subtypes, and not be universally expressed in any subtype. Among liposarcoma and leiomyosarcoma, the two most common adult soft tissue sarcoma subtypes, approximately 40% are Rb-positive, with an enrichment in the well-differentiated liposarcoma histology for Rb expression compared with the dedifferentiated or myxoid subtypes (90%–100% IHC positive in well-differentiated, versus 33% in dedifferentiated and 0% in myxoid) (14, 40–42). This heterogeneity in the pattern of Rb expression by histologic subtype suggests that screening for expression of Rb will be necessary for trial enrollment to enrich for potential responders. Osteosarcoma, the most common childhood sarcoma, also may be a good candidate for this therapy, as 50% are Rb positive, and p16 is frequently hypermethylated (43). Our *in vitro* data (Figure 1) showing that RD cells with very low levels of Rb levels are not responsive to palbociclib, raises the possibility that there may be a threshold of Rb activity that is needed for palbociclib to mediate its growth inhibitory (i.e G1 arrest) activity. Unlike Rb, where there is consensus among different tumor types regarding the predictive value of this protein, it remains controversial as to whether CDK4 or CDK6 levels may be useful in selecting patients for CDK4/6 inhibitor based therapy. In one preclinical study using a different CDK4/6 inhibitor (LEE011), CDK4 amplification in rhabdomyosarcoma was shown to be a biomarker of resistance due to inability to activate the G1 checkpoint and induce G1 arrest (44). However,

another recent study showed that in other soft tissue sarcomas (cell lines and PDXs), those with high levels of CDK4 were more sensitive compared to low-expressing tumors (45).

A concern with using drugs such as palbociclib to induce G1 arrest and then allowing for a period of recovery is that normal cycling tissues may also be affected, making them more sensitive to subsequent DNA damage and cell death. However, this should not be the case due to the presence of intact G1 and G2 checkpoints and wild-type p53 in normal tissues. In mice it has recently been shown that CDK4/6 inhibition protected normal intestinal epithelium from radiation-induced damage, through the inhibition of radiation-induced p53 activation (46). In normal hematopoietic cells, non-selective cell cycle inhibition with cyclohexamide was able to protect them from Ara-C toxicity, while leukemic cells were not protected, again suggesting that the basal differences in cell cycle between normal and tumor cells provides a therapeutic window for the use of smart combination treatment strategies (47).

Combination therapies are often necessary to treat aggressive tumors such as sarcomas, and palbociclib may be an ideal drug to consider for other combinations. Indeed, in a large screen of PDX models, LEE011 (Novartis CDK4/6 inhibitor) synergized with several different signal transduction pathway targeting agents, based on the premise that targeting a single pathway more potently leads to more resistance (48). Recent work has identified that the PI3K pathway may be a mechanism of resistance to palbociclib in breast cancer, making the argument that co-targeting PI3K may be beneficial (49). In osteosarcoma particularly, it is known that this pathway is a therapeutic vulnerability, making a triple combination strategy (CDK4/6, Wee1 and mTOR) possible since mTOR inhibitors do not have overlapping toxicities with CDK4/6 and Wee1 kinase inhibitors (50).

Our study adds to the growing literature that sequencing matters to the effectiveness of combination therapies in cancer, both in terms of tumor cell cytotoxicity as well as minimizing normal tissue damage. Our group has previously identified that CDK1/2 inhibition prior to doxorubicin selectively targets triple-negative breast cancer cells for DNA-damage-induced cell death in a mutant p53-dependent manner, through CDK1-mediated inhibition of DNA repair (51). Previous work on palbociclib in breast cancer cells expressing Rb has demonstrated that concomitant treatment with anthracyclines is antagonistic, as would be expected due to G1 arrest (52). In ovarian cancer models, sequential palbociclib and chemotherapy (carboplatin or paclitaxel) without recovery was also shown to be antagonistic (53). Our work shows however, that in Rb-positive sarcomas, palbociclib and doxorubicin can be combined successfully by allowing a period of recovery in between, indicating that sequence, drug stability/half-life, mechanism of action and timing of drug delivery must be considered when designing combination treatments.

Supplementary Material

Refer to Web version on PubMed Central for supplementary material.

Acknowledgments

Financial Information

This work was supported by a Department of Defense Breast Cancer Research Program Postdoctoral Fellowship (BC112270 to A. Alexander), and T32 Fellowship (CA009599 to A.M. Frqancis), National Institutes of Health grants CA87458 and CA1522228, a Sarcoma Foundation of America grant, and a joint grant from Alan B. Slifka and National Leiomyosarcoma Research Foundations (to K. Keyomarsi) and John Wayne Cancer Foundation (to K.K. Hunt). Institutional resources utilized included the Characterized Cell Line Core Facility and the Flow Cytometry and Cellular Imaging Facility, which are supported in part by the National Institutes of Health through MD Anderson's Cancer Center Support Grant CA016672 (to K. Keyomarsi and K.K. Hunt, co-leaders of the Breast Program).

References

1. Dancsok AR, Asleh-Aburaya K, Nielsen TO. Advances in sarcoma diagnostics and treatment. Oncotarget. 2016
2. Williams RF, Fernandez-Pineda I, Gosain A. Pediatric Sarcomas. Surg Clin North Am. 2016; 96:1107–25. [PubMed: 27542645]
3. Bajpai J, Susan D. Adjuvant chemotherapy in soft tissue sarcomas…Conflicts, consensus, and controversies. South Asian J Cancer. 2016; 5:15–9. [PubMed: 27169114]
4. Gladdy RA, Gupta A, Catton CN. Retroperitoneal Sarcoma: Fact, Opinion, and Controversy. Surg Oncol Clin N Am. 2016; 25:697–711. [PubMed: 27591493]
5. Burningham Z, Hashibe M, Spector L, Schiffman JD. The epidemiology of sarcoma. Clin Sarcoma Res. 2012; 2:14. [PubMed: 23036164]
6. Larrier NA, Czito BG, Kirsch DG. Radiation Therapy for Soft Tissue Sarcoma: Indications and Controversies for Neoadjuvant Therapy, Adjuvant Therapy, Intraoperative Radiation Therapy, and Brachytherapy. Surg Oncol Clin N Am. 2016; 25:841–60. [PubMed: 27591502]
7. Helman LJ, Meltzer P. Mechanisms of sarcoma development. Nat Rev Cancer. 2003; 3:685–94. [PubMed: 12951587]
8. Mackall CL, Meltzer PS, Helman LJ. Focus on sarcomas. Cancer Cell. 2002; 2:175–8. [PubMed: 12242149]
9. Henderson-Jackson EB, Bui MM. Molecular Pathology of Soft-Tissue Neoplasms and Its Role in Clinical Practice. Cancer Control. 2015; 22:186–92. [PubMed: 26068763]
10. Cranmer LD, Loggers ET, Pollack SM. Pazopanib in the management of advanced soft tissue sarcomas. Ther Clin Risk Manag. 2016; 12:941–55. [PubMed: 27354810]
11. Mir O, Cropet C, Toulmonde M, Cesne AL, Molimard M, Bompas E, Cassier P, Ray-Coquard I, Rios M, Adenis A, Italiano A, Bouché O, Chauzit E, Duffaud F, Bertucci F, Isambert N, Gautier J, Blay JY, Pérol D. (GSF-GETO) PsgotFSG-GdEdTO. Pazopanib plus best supportive care versus best supportive care alone in advanced gastrointestinal stromal tumours resistant to imatinib and sunitinib (PAZOGIST): a randomised, multicentre, open-label phase 2 trial. Lancet Oncol. 2016; 17:632–41. [PubMed: 27068858]
12. Nishida T, Doi T. Pazopanib for both GIST and soft-tissue sarcoma. Lancet Oncol. 2016; 17:549–50. [PubMed: 27068859]
13. Liao Y, Feng Y, Shen J, Hornicek FJ, Duan Z. The roles and therapeutic potential of cyclin-dependent kinases (CDKs) in sarcoma. Cancer Metastasis Rev. 2016; 35:151–63. [PubMed: 26669603]
14. Sabah M, Cummins R, Leader M, Kay E. Aberrant expression of the Rb pathway proteins in soft tissue sarcomas. Appl Immunohistochem Mol Morphol. 2006; 14:397–403. [PubMed: 17122635]
15. Beaver JA, Amiri-Kordestani L, Charlab R, Chen W, Palmby T, Tilley A, Zirkelbach JF, Yu J, Liu Q, Zhao L, Crich J, Chen XH, Hughes M, Bloomquist E, Tang S, Sridhara R, Kluetz PG, Kim G, Ibrahim A, Pazdur R, Cortazar P. FDA Approval: Palbociclib for the Treatment of Postmenopausal Patients with Estrogen Receptor-Positive, HER2-Negative Metastatic Breast Cancer. Clin Cancer Res. 2015; 21:4760–6. [PubMed: 26324739]
16. Walker AJ, Wedam S, Amiri-Kordestani L, Bloomquist E, Tang S, Sridhara R, Chen W, Palmby TR, Fourie Zirkelbach J, Fu W, Liu Q, Tilley A, Kim G, Kluetz PG, McKee AE, Pazdur R. FDA Approval of Palbociclib in Combination with Fulvestrant for the Treatment of Hormone Receptor-Positive, HER2-Negative Metastatic Breast Cancer. Clin Cancer Res. 2016; 22:4968–72. [PubMed: 27407089]

17. Barroso-Sousa R, Shapiro GI, Tolaney SM. Clinical Development of the CDK4/6 Inhibitors Ribociclib and Abemaciclib in Breast Cancer. Breast Care (Basel). 2016; 11:167–73. [PubMed: 27493615]

18. VanArsdale T, Boshoff C, Arndt KT, Abraham RT. Molecular Pathways: Targeting the Cyclin D-CDK4/6 Axis for Cancer Treatment. Clin Cancer Res. 2015; 21:2905–10. [PubMed: 25941111]

19. Lim JS, Turner NC, Yap TA. CDK4/6 Inhibitors: Promising Opportunities beyond Breast Cancer. Cancer Discov. 2016; 6:697–9. [PubMed: 27371575]

20. Zhang YX, Sicinska E, Czaplinski JT, Remillard SP, Moss S, Wang Y, Brain C, Loo A, Snyder EL, Demetri GD, Kim S, Kung AL, Wagner AJ. Antiproliferative effects of CDK4/6 inhibition in CDK4-amplified human liposarcoma in vitro and in vivo. Mol Cancer Ther. 2014; 13:2184–93. [PubMed: 25028469]

21. Dickson MA, Tap WD, Keohan ML, D'Angelo SP, Gounder MM, Antonescu CR, Landa J, Qin LX, Rathbone DD, Condy MM, Ustoyev Y, Crago AM, Singer S, Schwartz GK. Phase II trial of the CDK4 inhibitor PD0332991 in patients with advanced CDK4-amplified well-differentiated or dedifferentiated liposarcoma. J Clin Oncol. 2013; 31:2024–8. [PubMed: 23569312]

22. Dickson MA, Schwartz GK, Keohan ML, D'Angelo SP, Gounder MM, Chi P, Antonescu CR, Landa J, Qin LX, Crago AM, Singer S, Koff A, Tap WD. Progression-Free Survival Among Patients With Well-Differentiated or Dedifferentiated Liposarcoma Treated With CDK4 Inhibitor Palbociclib: A Phase 2 Clinical Trial. JAMA Oncol. 2016; 2:937–40. [PubMed: 27124835]

23. Aarts M, Sharpe R, Garcia-Murillas I, Gevensleben H, Hurd MS, Shumway SD, Toniatti C, Ashworth A, Turner NC. Forced mitotic entry of S-phase cells as a therapeutic strategy induced by inhibition of WEE1. Cancer Discov. 2012; 2:524–39. [PubMed: 22628408]

24. Hirai H, Iwasawa Y, Okada M, Arai T, Nishibata T, Kobayashi M, Kimura T, Kaneko N, Ohtani J, Yamanaka K, Itadani H, Takahashi-Suzuki I, Fukasawa K, Oki H, Nambu T, Jiang J, Sakai T, Arakawa H, Sakamoto T, Sagara T, Yoshizumi T, Mizuarai S, Kotani H. Small-molecule inhibition of Wee1 kinase by MK-1775 selectively sensitizes p53-deficient tumor cells to DNA-damaging agents. Mol Cancer Ther. 2009; 8:2992–3000. [PubMed: 19887545]

25. Finn RS, Dering J, Conklin D, Kalous O, Cohen DJ, Desai AJ, Ginther C, Atefi M, Chen I, Fowst C, Los G, Slamon DJ. PD 0332991, a selective cyclin D kinase 4/6 inhibitor, preferentially inhibits proliferation of luminal estrogen receptor-positive human breast cancer cell lines in vitro. Breast Cancer Res. 2009; 11:R77. [PubMed: 19874578]

26. Nanos-Webb A, Jabbour NA, Multani AS, Wingate H, Oumata N, Galons H, Joseph B, Meijer L, Hunt KK, Keyomarsi K. Targeting low molecular weight cyclin E (LMW-E) in breast cancer. Breast Cancer Res Treat. 2012; 132:575–88. [PubMed: 21695458]

27. Finn RS, Dering J, Conklin D, Kalous O, Cohen DJ, Desai AJ, Ginther C, Atefi M, Chen I, Fowst C, Los G, Slamon DJ. PD 0332991, a selective cyclin D kinase 4/6 inhibitor, preferentially inhibits proliferation of luminal estrogen receptor-positive human breast cancer cell lines in vitro. Breast cancer research : BCR. 2009; 11:R77. [PubMed: 19874578]

28. Sherr CJ, Beach D, Shapiro GI. Targeting CDK4 and CDK6: From Discovery to Therapy. Cancer Discov. 2016; 6:353–67. [PubMed: 26658964]

29. Flaherty KT, Lorusso PM, Demichele A, Abramson VG, Courtney R, Randolph SS, Shaik MN, Wilner KD, O'Dwyer PJ, Schwartz GK. Phase I, dose-escalation trial of the oral cyclin-dependent kinase 4/6 inhibitor PD 0332991, administered using a 21-day schedule in patients with advanced cancer. Clin Cancer Res. 2012; 18:568–76. [PubMed: 22090362]

30. Chou T-C, Talalay P. Analysis of combined drug effects: a new look at a very old problem. Trends in Pharmacological Sciences. 1983; 4:450–4.

31. Vora SR, Juric D, Kim N, Mino-Kenudson M, Huynh T, Costa C, Lockerman EL, Pollack SF, Liu M, Li X, Lehar J, Wiesmann M, Wartmann M, Chen Y, Cao ZA, Pinzon-Ortiz M, Kim S, Schlegel R, Huang A, Engelman JA. CDK 4/6 inhibitors sensitize PIK3CA mutant breast cancer to PI3K inhibitors. Cancer Cell. 2014; 26:136–49. [PubMed: 25002028]

32. Taylor-Harding B, Aspuria PJ, Agadjanian H, Cheon DJ, Mizuno T, Greenberg D, Allen JR, Spurka L, Funari V, Spiteri E, Wang Q, Orsulic S, Walsh C, Karlan BY, Wiedemeyer WR. Cyclin E1 and RTK/RAS signaling drive CDK inhibitor resistance via activation of E2F and ETS. Oncotarget. 2015; 6:696–714. [PubMed: 25557169]

33. Adriamycin FDA package insert. [cited; Available from: http://www.accessdata.fda.gov/drugsatfda_docs/label/2012/062921s022lbl.pdf
34. Do K, Wilsker D, Ji J, Zlott J, Freshwater T, Kinders RJ, Collins J, Chen AP, Doroshow JH, Kummar S. Phase I Study of Single-Agent AZD1775 (MK-1775), a Wee1 Kinase Inhibitor, in Patients With Refractory Solid Tumors. J Clin Oncol. 2015; 33:3409–15. [PubMed: 25964244]
35. Vlenterie M, Hillebrandt-Roeffen MH, Schaars EW, Flucke UE, Fleuren ED, Navis AC, Leenders WP, Versleijen-Jonkers YM, van der Graaf WT. Targeting Cyclin-Dependent Kinases in Synovial Sarcoma: Palbociclib as a Potential Treatment for Synovial Sarcoma Patients. Ann Surg Oncol. 2016; 23:2745–52. [PubMed: 27334220]
36. Liu L, Wu J, Ong SS, Chen T. Cyclin-dependent kinase 4 phosphorylates and positively regulates PAX3-FOXO1 in human alveolar rhabdomyosarcoma cells. PLoS One. 2013; 8:e58193. [PubMed: 23469153]
37. Desar IM, Constantinidou A, Kaal SE, Jones RL, van der Graaf WT. Advanced soft-tissue sarcoma and treatment options: critical appraisal of trabectedin. Cancer Manag Res. 2016; 8:95–104. [PubMed: 27574465]
38. Tap WD, Jones RL, Van Tine BA, Chmielowski B, Elias AD, Adkins D, Agulnik M, Cooney MM, Livingston MB, Pennock G, Hameed MR, Shah GD, Qin A, Shahir A, Cronier DM, Ilaria R, Conti I, Cosaert J, Schwartz GK. Olaratumab and doxorubicin versus doxorubicin alone for treatment of soft-tissue sarcoma: an open-label phase 1b and randomised phase 2 trial. Lancet. 2016; 388:488–97. [PubMed: 27291997]
39. Pang A, Carbini M, Maki RG. Contemporary Therapy for Advanced Soft-Tissue Sarcomas in Adults: A Review. JAMA Oncol. 2016; 2:941–7. [PubMed: 27148906]
40. Wang T, Goodman MA, McGough RL, Weiss KR, Rao UN. Immunohistochemical analysis of expressions of RB1, CDK4, HSP90, cPLA2G4A, and CHMP2B is helpful in distinction between myxofibrosarcoma and myxoid liposarcoma. Int J Surg Pathol. 2014; 22:589–99. [PubMed: 24788530]
41. Takahira T, Oda Y, Tamiya S, Yamamoto H, Kobayashi C, Izumi T, Ito K, Iwamoto Y, Tsuneyoshi M. Alterations of the RB1 gene in dedifferentiated liposarcoma. Mod Pathol. 2005; 18:1461–70. [PubMed: 15933756]
42. Schneider-Stock R, Boltze C, Jaeger V, Stumm M, Seiler C, Rys J, Schütze K, Roessner A. Significance of loss of heterozygosity of the RB1 gene during tumour progression in well-differentiated liposarcomas. J Pathol. 2002; 197:654–60. [PubMed: 12210086]
43. Benassi MS, Molendini L, Gamberi G, Ragazzini P, Sollazzo MR, Merli M, Asp J, Magagnoli G, Balladelli A, Bertoni F, Picci P. Alteration of pRb/p16/cdk4 regulation in human osteosarcoma. Int J Cancer. 1999; 84:489–93. [PubMed: 10502725]
44. Olanich ME, Sun W, Hewitt SM, Abdullaev Z, Pack SD, Barr FG. CDK4 Amplification Reduces Sensitivity to CDK4/6 Inhibition in Fusion-Positive Rhabdomyosarcoma. Clin Cancer Res. 2015; 21:4947–59. [PubMed: 25810375]
45. Perez M, Muñoz-Galván S, Jiménez-García MP, Marín JJ, Carnero A. Efficacy of CDK4 inhibition against sarcomas depends on their levels of CDK4 and p16ink4 mRNA. Oncotarget. 2015; 6:40557–74. [PubMed: 26528855]
46. Wei L, Leibowitz BJ, Wang X, Epperly M, Greenberger J, Zhang L, Yu J. Inhibition of CDK4/6 protects against radiation-induced intestinal injury in mice. J Clin Invest. 2016; 126:4076–87. [PubMed: 27701148]
47. Slapak CA, Fine RL, Richman CM. Differential protection of normal and malignant human myeloid progenitors (CFU-GM) from Ara-C toxicity using cycloheximide. Blood. 1985; 66:830–4. [PubMed: 3862435]
48. Gao H, Korn JM, Ferretti S, Monahan JE, Wang Y, Singh M, Zhang C, Schnell C, Yang G, Zhang Y, Balbin OA, Barbe S, Cai H, Casey F, Chatterjee S, Chiang DY, Chuai S, Cogan SM, Collins SD, Dammassa E, Ebel N, Embry M, Green J, Kauffmann A, Kowal C, Leary RJ, Lehar J, Liang Y, Loo A, Lorenzana E, Robert McDonald E, McLaughlin ME, Merkin J, Meyer R, Naylor TL, Patawaran M, Reddy A, Röelli C, Ruddy DA, Salangsang F, Santacroce F, Singh AP, Tang Y, Tinetto W, Tobler S, Velazquez R, Venkatesan K, Von Arx F, Wang HQ, Wang Z, Wiesmann M, Wyss D, Xu F, Bitter H, Atadja P, Lees E, Hofmann F, Li E, Keen N, Cozens R, Jensen MR, Pryer

NK, Williams JA, Sellers WR. High-throughput screening using patient-derived tumor xenografts to predict clinical trial drug response. Nat Med. 2015; 21:1318–25. [PubMed: 26479923]

49. Herrera-Abreu MT, Palafox M, Asghar U, Rivas MA, Cutts RJ, Garcia-Murillas I, Pearson A, Guzman M, Rodriguez O, Grueso J, Bellet M, Cortes J, Elliott R, Pancholi S, Baselga J, Dowsett M, Martin LA, Turner NC, Serra V. Early Adaptation and Acquired Resistance to CDK4/6 Inhibition in Estrogen Receptor-Positive Breast Cancer. Cancer Res. 2016; 76:2301–13. [PubMed: 27020857]
50. Perry JA, Kiezun A, Tonzi P, Van Allen EM, Carter SL, Baca SC, Cowley GS, Bhatt AS, Rheinbay E, Pedamallu CS, Helman E, Taylor-Weiner A, McKenna A, DeLuca DS, Lawrence MS, Ambrogio L, Sougnez C, Sivachenko A, Walensky LD, Wagle N, Mora J, de Torres C, Lavarino C, Dos Santos Aguiar S, Yunes JA, Brandalise SR, Mercado-Celis GE, Melendez-Zajgla J, Cárdenas-Cardós R, Velasco-Hidalgo L, Roberts CW, Garraway LA, Rodriguez-Galindo C, Gabriel SB, Lander ES, Golub TR, Orkin SH, Getz G, Janeway KA. Complementary genomic approaches highlight the PI3K/mTOR pathway as a common vulnerability in osteosarcoma. Proc Natl Acad Sci U S A. 2014; 111:E5564–73. [PubMed: 25512523]
51. Jabbour-Leung NA, Chen X, Bui T, Jiang Y, Yang D, Vijayaraghavan S, McArthur MJ, Hunt KK, Keyomarsi K. Sequential Combination Therapy of CDK Inhibition and Doxorubicin Is Synthetically Lethal in p53-Mutant Triple-Negative Breast Cancer. Mol Cancer Ther. 2016; 15:593–607. [PubMed: 26826118]
52. McClendon AK, Dean JL, Rivadeneira DB, Yu JE, Reed CA, Gao E, Farber JL, Force T, Koch WJ, Knudsen ES. CDK4/6 inhibition antagonizes the cytotoxic response to anthracycline therapy. Cell Cycle. 2012; 11:2747–55. [PubMed: 22751436]
53. Konecny GE, Winterhoff B, Kolarova T, Qi J, Manivong K, Dering J, Yang G, Chalukya M, Wang HJ, Anderson L, Kalli KR, Finn RS, Ginther C, Jones S, Velculescu VE, Riehle D, Cliby WA, Randolph S, Koehler M, Hartmann LC, Slamon DJ. Expression of p16 and retinoblastoma determines response to CDK4/6 inhibition in ovarian cancer. Clin Cancer Res. 2011; 17:1591–602. [PubMed: 21278246]

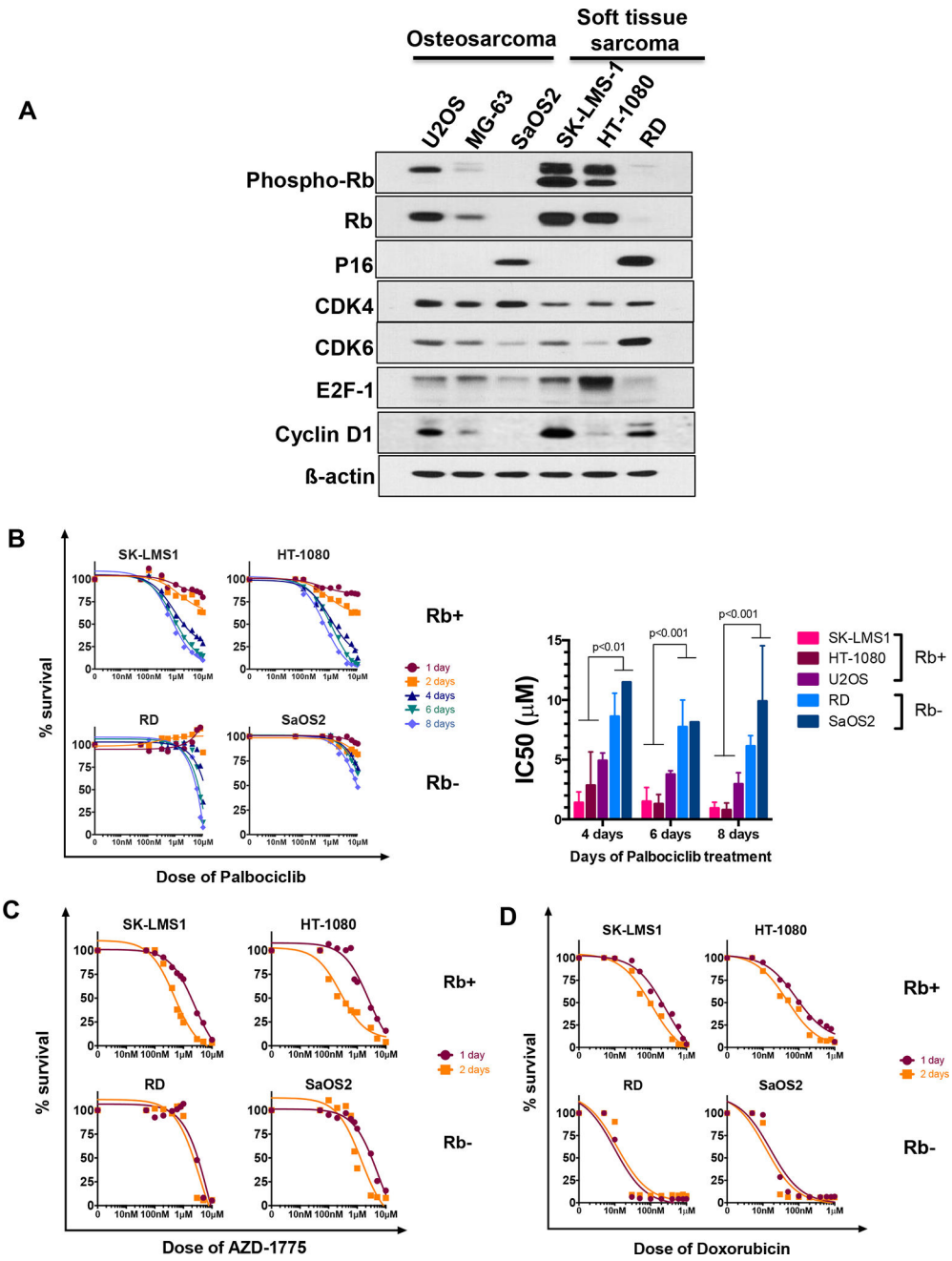

Figure 1. G1 checkpoint characterization and sensitivity to drug treatments

(A) Western blots for indicated proteins, using actin as a loading control. These blots show that SK-LMS1 and HT-1080 are Rb-positive, and therefore represent ideal models for evaluating CDK4/6 inhibitor-based therapy. (B) Sensitivity of sarcoma cell lines to palbociclib treatment for 1–8 days as indicated, measured by MTT on day 13. Graph shows IC50 for each cell line as a function of length of treatment (n=2–4 experiments). (C) Sensitivity of sarcoma cell lines to treatment with Wee1 kinase inhibitor (AZD1775) for 1 or 2 days (n=2 experiments). MTT was performed on day 12/13 to measure survival proportion. (D) Sensitivity of 4 sarcoma cell lines to 1 or 2 days of treatment with

doxorubicin (n=2 experiments). MTT was performed on day 12/13 to measure survival proportion.

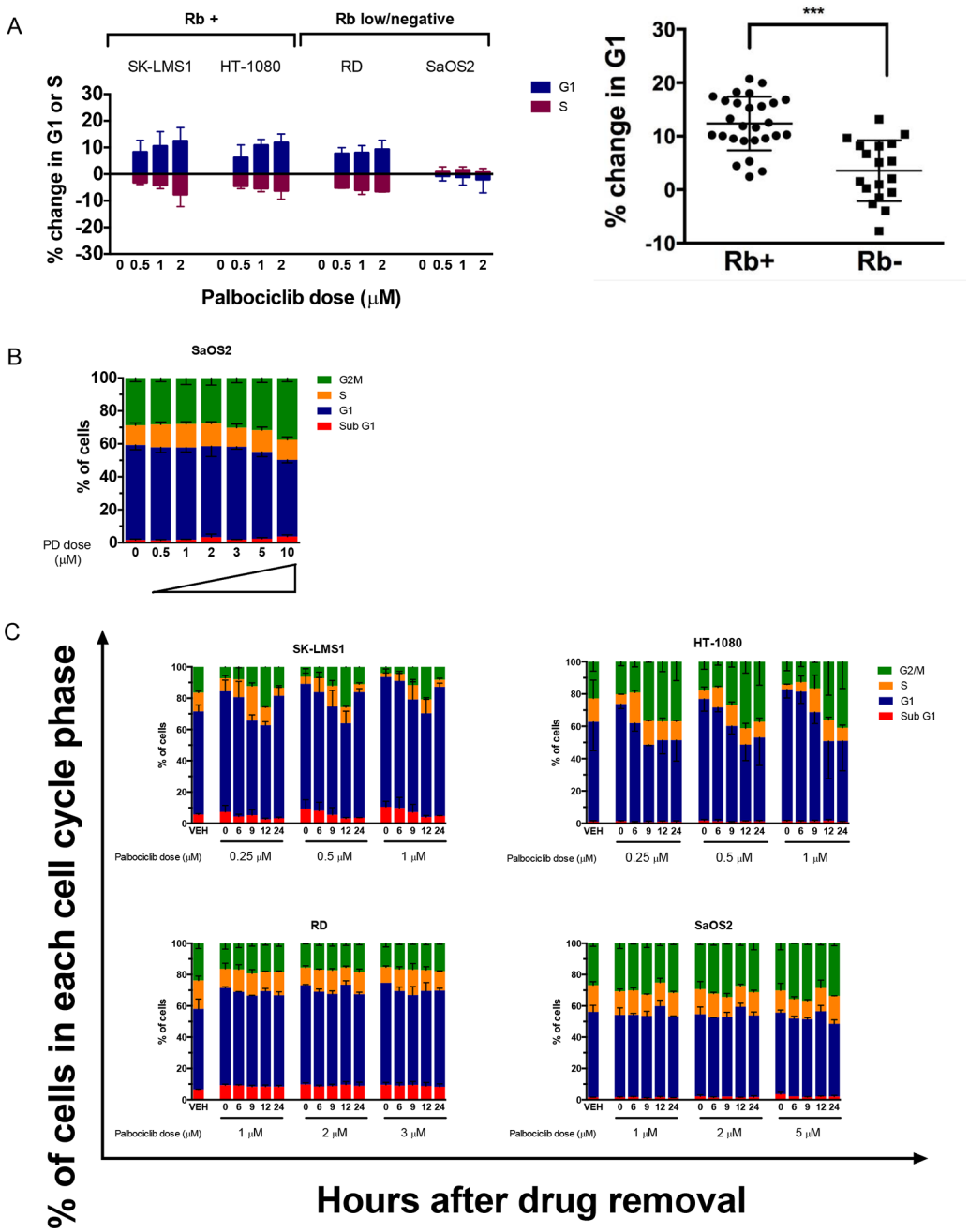

Figure 2. Palbociclib induces a reversible G1 arrest only in Rb-positive cell lines

(A) Percentage change in proportion of cells in G1 or S phase in the cell cycle after 6 days of treatment with the indicated concentrations of palbociclib for 6 days, normalized to the vehicle (DMSO). The right panel shows the results for all 5 cell lines, dichotomized into Rb-positive (SK-LMS1, HT-1080, U2OS) versus Rb-negative (RD, SaOS2),*** $p<0.0001$ (t-test). (B) Cell cycle distribution of SaOS2 cells treated with a wider range of palbociclib doses for 6 days prior to fixation and staining with PI (n=3). (C) Kinetics of cell cycle progression post-removal of palbociclib treatments as indicated (n=2). Cells were plated, treated with palbociclib for 6 days at the indicated doses, and then fresh media was added

for the different periods of time as labeled. Fixed cells were stained all together (for each experiment) with PI and analyzed by flow cytometry.

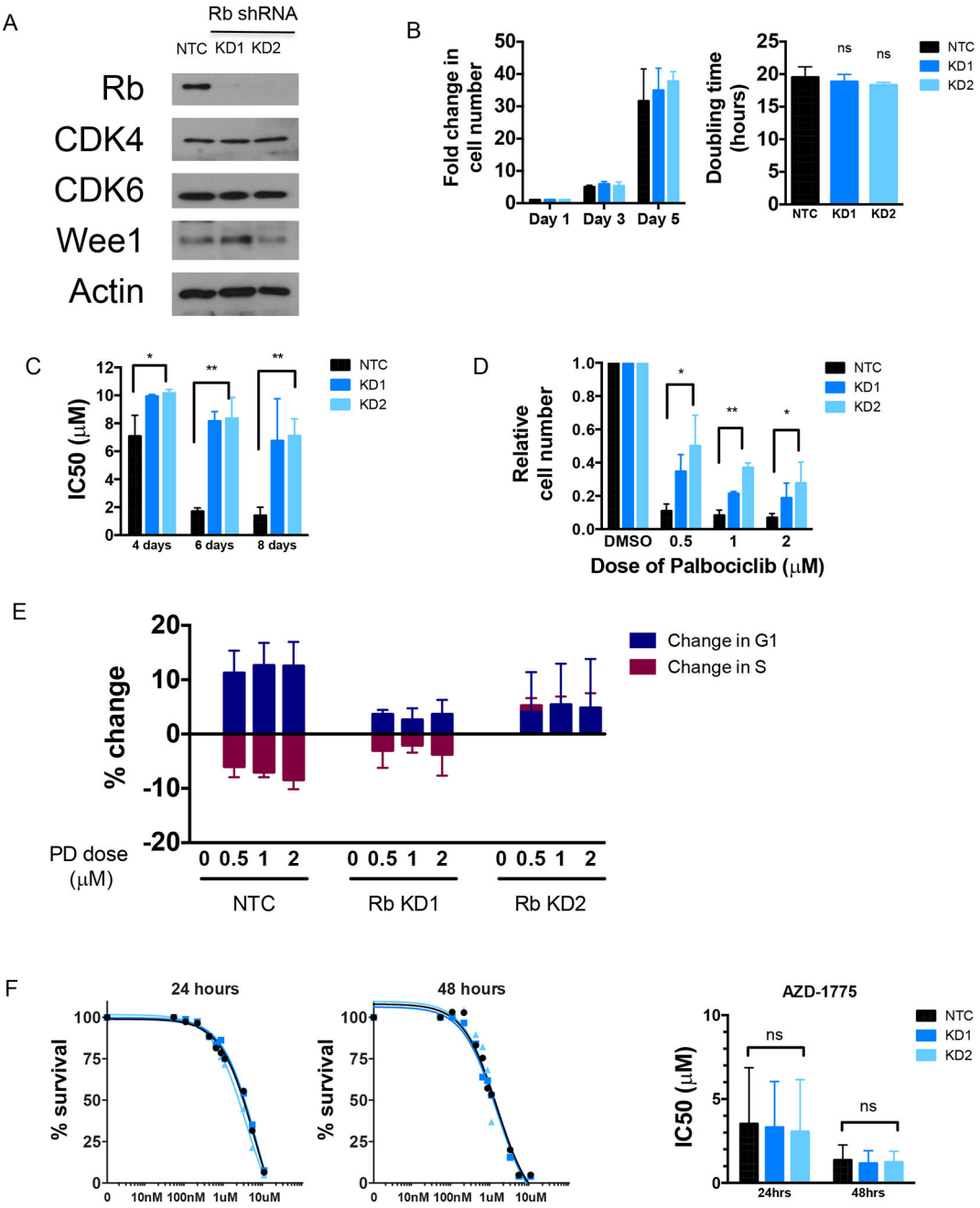

Figure 3. Rb knockdown induces palbociclib resistance

(A) Western blot showing successful knockdown of Rb and indicated proteins in SK-LMS1 cells expressing non-targeting control (NTC) shRNA or Rb shRNA. Rb is significantly depleted, while other drug targets are not significantly altered. Actin serves as a loading control on the gels. (B) Cell number after indicated number of days and doubling time (ns = not significant compared to NTC). (C) IC50 for 4, 6 and 8 days of palbociclib treatment in SK-LMS1 cells, using MTT as a readout of survival at day 12 (n=3), *p < 0.05, **p < 0.01. (D) Cell number after 6 days of palbociclib treatment with the indicated doses, normalized to vehicle in each cell line (DMSO) (n=3), *p < 0.05 (NTC vs KD1+KD2), **p < 0.01

(NTC vs KD1+KD2). (E) Cell cycle change in G1 and S phase for cells treated with palbociclib for 6 days prior to fixation and flow cytometry analysis. (F) Sensitivity to AZD1775 treatment for 24 or 48 hours using MTT as a readout of survival at day 12/13 (n=2). Right panel shows IC50 values derived from the individual experiments, ns = not significant.

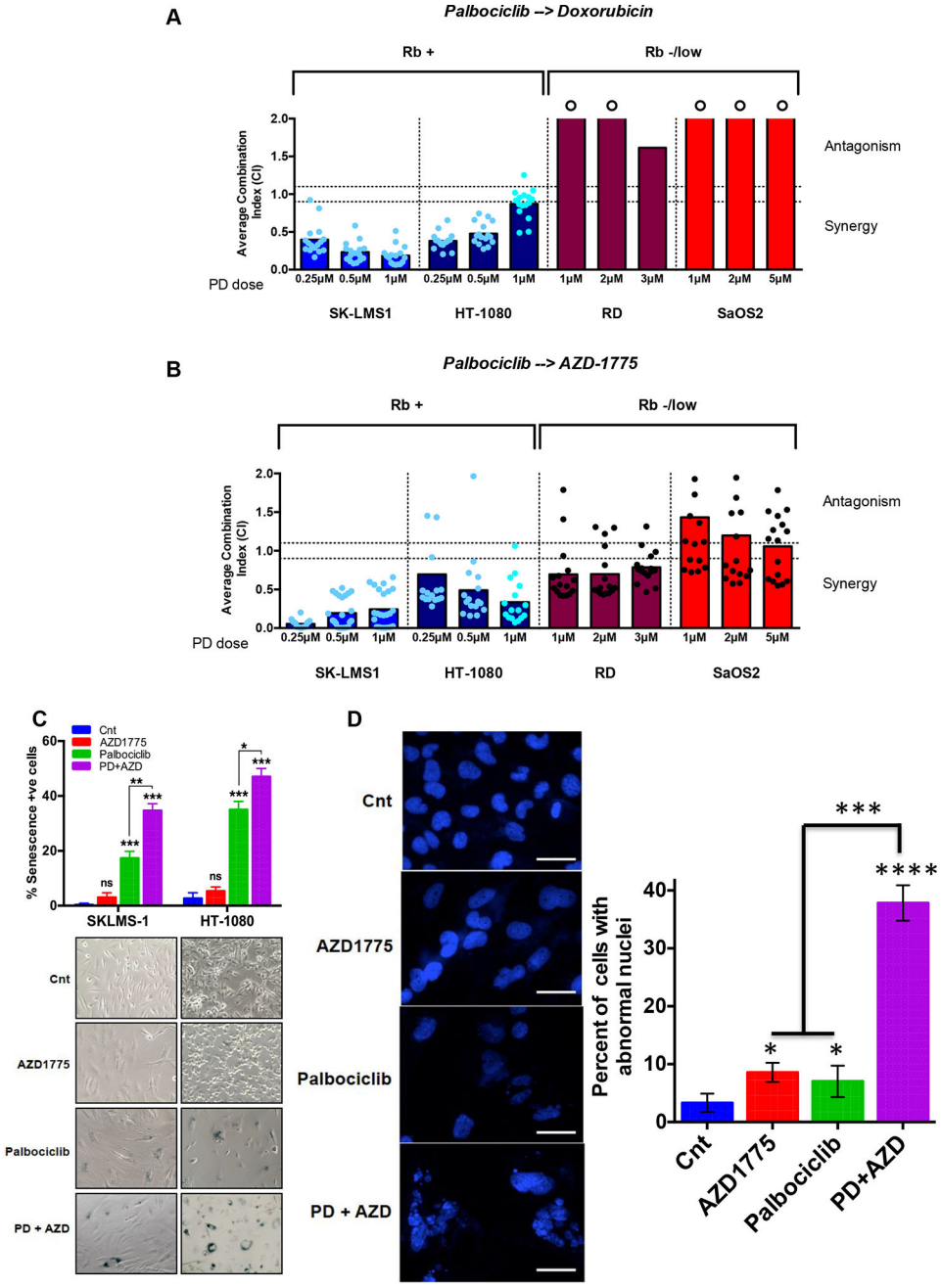

Figure 4. Combination treatment with palbociclib followed by doxorubicin or Wee1 inhibitor is synergistic in Rb-positive sarcoma cell lines

(A) Average combination index (CI) for sequential treatment with palbociclib for 6 days, followed by recovery for 9 hrs (except HT-1080 which was 6 hrs) and doxorubicin or (B) AZD1775 for 2 days. Survival was quantified using MTT on day 12 and survival fraction data were input into CalcuSyn software to generate the CI. Each dot represents one of the pairs of drug concentrations. Dotted lines represent the CI range of additivity (0.9–1.1), antagonism (>1.1) or synergism (<0.9). A circle above a bar means that the CI exceeds 2 but was capped at 2 for data presentation. (C) SA-β galactosidase activity measurement (top) with representative images (bottom) of SKLMS-1 and HT1080 cells treated with palbociclib

(6 days) followed by 9 hrs (SKLMS) or 6 hrs (HT1080) recovery followed by AZD1775 (2 days). (D) Representative images of DAPI staining (left) and quantitation (right) of SK-LMS1 cells treated with palbociclib for 9 days, then allowed to recover for 9 hrs followed by 48 hrs of AZD treatment. Single drug treatments were performed in parallel either in the absence of palbociclib or AZD. At the end of treatment, cells were fixed with methanol and stained with DAPI to visualize nuclear morphology. Scale bars equal 50 μ. A minimum of 150 cells (per condition) were scored for abnormal nuclear morphology. All data represent mean±SD from three independent experiments; p-values were calculated in comparison with control treated cells unless indicated otherwise, ns: $p>0.05$; *$p<0.05$; **$p<0.01$; ***$p<0.001$; ****$p<0.0001$

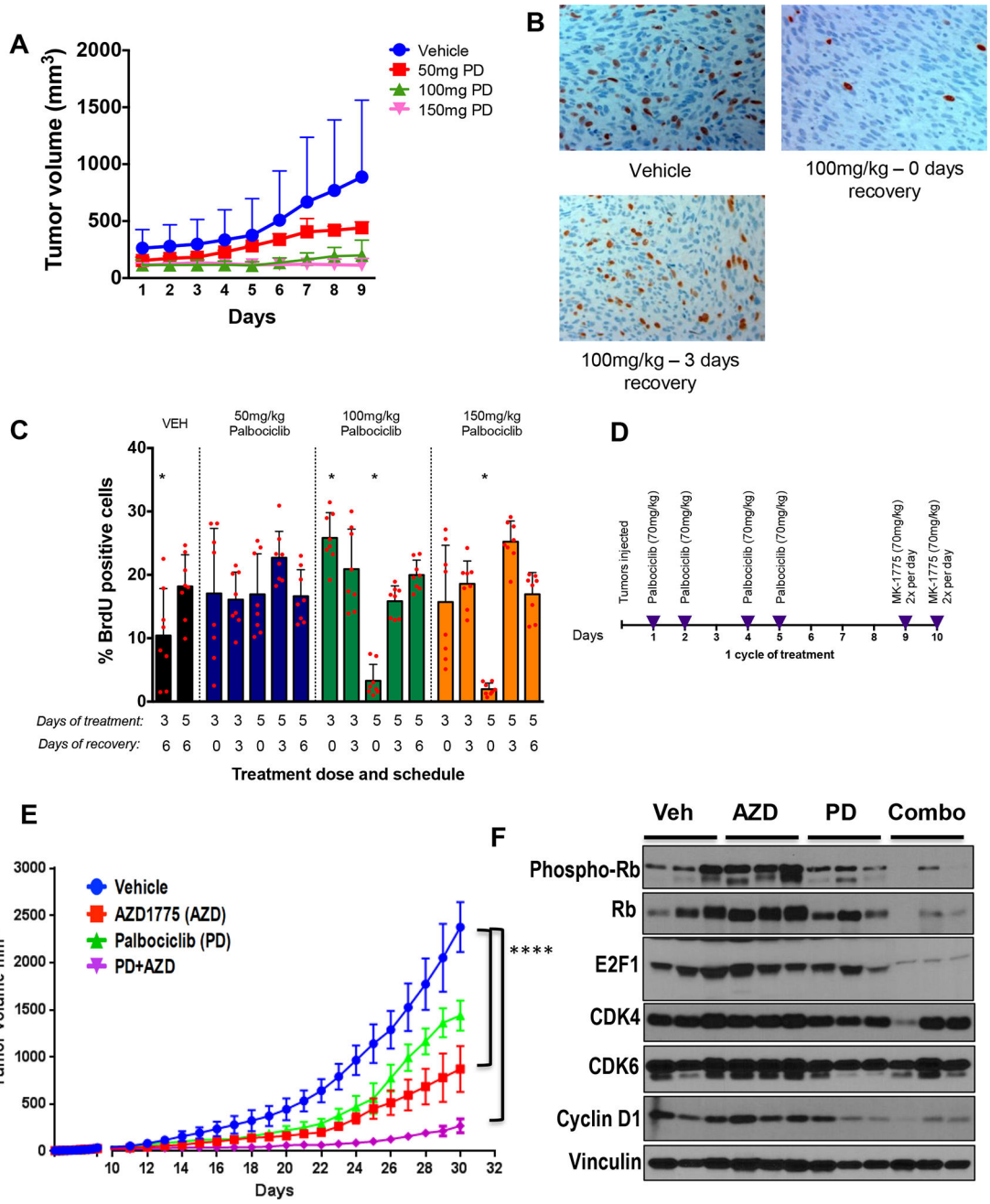

Figure 5. Optimization of *in vivo* treatment approach using SK-LMS1 xenografts

(A) Average tumor volumes for mice treated with vehicle, or the indicated doses of palbociclib daily for 6 days (n=2 per arm). Tumors were measured daily with calipers. (B) Representative BrdU IHC images showing reversibility of palbociclib-induced G1 arrest. (C) Proportion of BrdU positive cells under each treatment condition. The percentage of cells that were successfully labeled with BrdU was quantified manually using at least 2 images per slide, of which 400 cells per slide were counted as either positive or negative for BrdU staining for each mouse (n=3 mice per condition) for a total of 2,400 data points for each of the bar graphs presented. (D) Schematic showing treatment schedule for combination

treatment study. Palbociclib was given 4 times per week, on days 1, 2, 4 and 5 at a dose of 70 mg/kg, and AZD1775 treatment was twice per day, on days 9 and 10 to allow recovery after day 5 of palbociclib treatment. (E) Average SK-LMS1 tumor volume during treatment (n=9 vehicle arm, n=10 AZD arm, n=7 PD arm and n=7 for PD-AZD sequential combo), ****p <0.0001. (F) Western blot showing indicated proteins on tumor samples, using vinculin as a loading control. Phospho-Rb and cyclin D1 as a measure of palbociclib pharmacodynamics is significantly reduced in combination treated tumors. Levels of CDK4 and CDK6 are relatively stable across all treatment groups. Error bars represent the standard deviation from the mean, unless otherwise indicated. Pairwise comparisons were analyzed using multiple *t*-tests (one unpaired *t*-test per row).

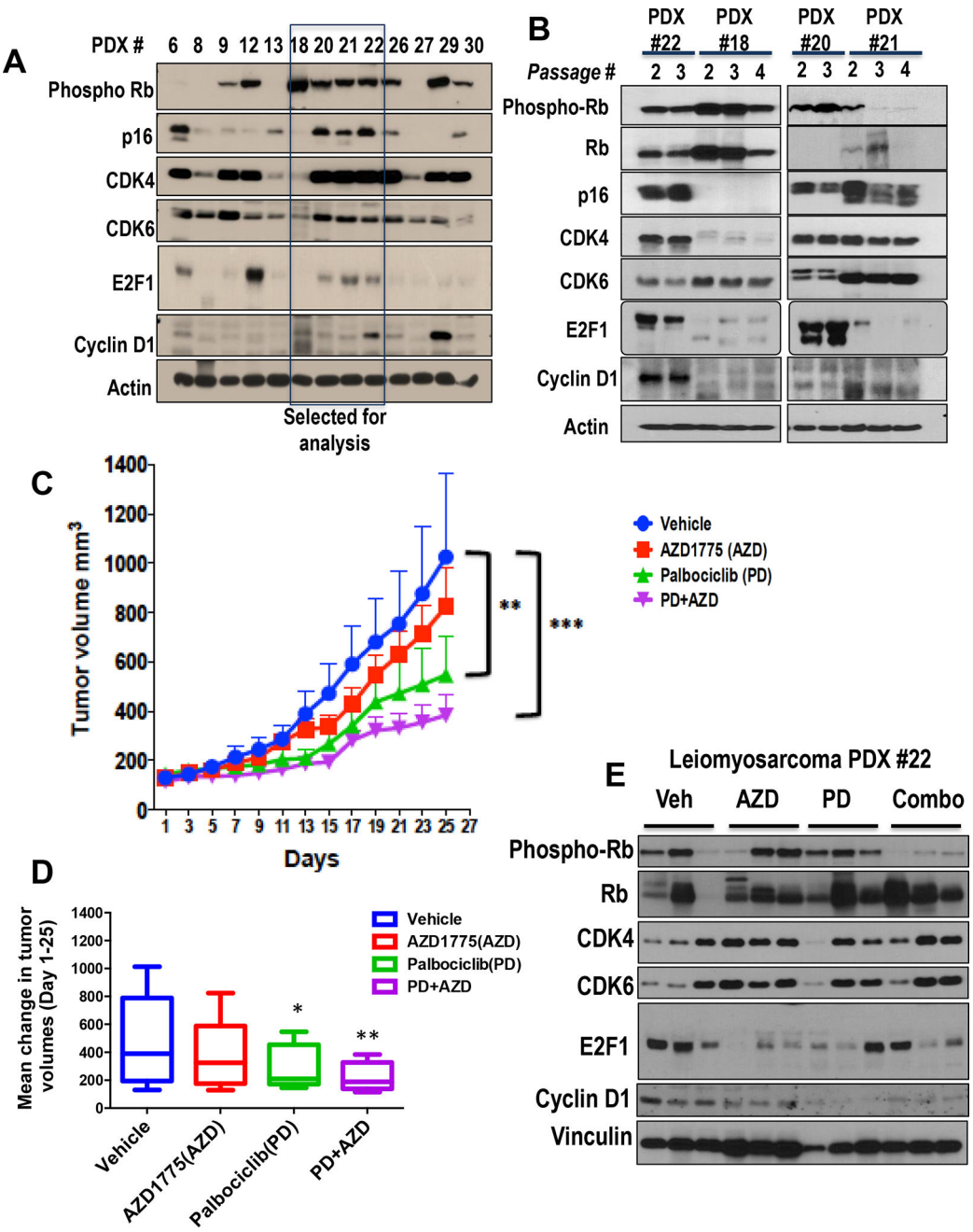

Figure 6. Combination treatment inhibits growth in an Rb-positive leiomyosarcoma PDX line

(A) Western blot analysis of 13 leiomyosarcoma PDX lines for G1 checkpoint proteins to select model for study. Four of the PDXs (PDX 18, 20, 21, 22) which were Rb-positive were chosen for further analysis. (B) Western blot analysis of Rb pathway proteins revealed stability across passages in untreated tumors. (C) Average PDX tumor volume (model #22) during treatment, (n=5 per arm for all). Each mouse in this study was implanted with the same passage of PDX#22 taken when the tumors reached the maximum size for sacrifice or the end of the experiment. Error bars represent SEM. (D) Mean fold change in PDX tumor volume between day 1 and day 25 (end of treatment). Error bars represent SEM. (E) Western

blot of tumor samples showing indicated proteins using vinculin as a loading control. Phospho-Rb and cyclin D1 as a measure of palbociclib pharmacodynamics are significantly reduced in combination treated tumors, while total Rb levels remain high. Levels of CDK4 and CDK6 are relatively stable across all treatment groups. Error bars represent the standard deviation from the mean unless otherwise indicated. Pairwise comparisons were analyzed using multiple *t*-tests (one unpaired *t*-test per row).